Evolution during Δ_1 yields:

$$\begin{aligned} d_{13}(5) &= d_{13}(4)\exp(-i\Omega_{13}\Delta_1) \\ &= -2i\exp(-i\Omega_H t_e)\exp[-i(\Omega_H+\pi J)\Delta_1] \\ &= -2i\exp[-i\Omega_H(t_e+\Delta_1)]\exp(-i\pi J\Delta_1) \end{aligned} \tag{I.27}$$

$$d_{24}(5) = -2i\exp[-i\Omega_H(t_e+\Delta_1)]\exp(+i\pi J\Delta_1) \tag{I.28}$$

To achieve our goal we choose $\Delta_1=1/2J$, which implies $\pi J\Delta_1=\pi/2$.

Using the expression [see (A16)]

$$\exp(\pm i\pi/2) = \cos(\pi/2) \pm i\sin(\pi/2) = \pm i$$

$$\begin{aligned} \exp(-i\pi J\Delta_1) &= -i \\ \exp(+i\pi J\Delta_1) &= +i \end{aligned} \tag{I.29}$$

We now have

$$\begin{aligned} d_{13}(5) &= -2\exp[-i\Omega_H(t_e+\Delta_1)] \\ d_{24}(5) &= +2\exp[-i\Omega_H(t_e+\Delta_1)] \end{aligned} \tag{I.30}$$

For the following calculations it is convenient to use the notations

$$\begin{aligned} c &= \cos[\Omega_H(t_e+\Delta_1)] \\ s &= \sin[\Omega_H(t_e+\Delta_1)] \end{aligned} \tag{I.31}$$

which lead to

$$\begin{aligned} d_{13}(5) &= -2(c-is) \\ d_{24}(5) &= +2(c-is) \end{aligned} \tag{I.32}$$

At this point the density matrix is:

$$D(5)=\begin{bmatrix} 3 & 0 & -2(c-is) & 0 \\ 0 & 2 & 0 & 2(c-is) \\ -2(c+is) & 0 & 3 & 0 \\ 0 & 2(c+is) & 0 & 2 \end{bmatrix} \quad \text{(I.33)}$$

3.8 Third and Fourth Pulses

Although physically these pulses are applied separately, we may save some calculation effort by treating them as a single nonselective pulse.

The expressions of R_{90xC} and R_{90xH} are taken from Appendix C.

$$R_{90xCH} = R_{90xC}R_{90xH}$$

$$=\frac{1}{\sqrt{2}}\begin{bmatrix} 1 & i & 0 & 0 \\ i & 1 & 0 & 0 \\ 0 & 0 & 1 & i \\ 0 & 0 & i & 1 \end{bmatrix}\frac{1}{\sqrt{2}}\begin{bmatrix} 1 & 0 & i & 0 \\ 0 & 1 & 0 & i \\ i & 0 & 1 & 0 \\ 0 & i & 0 & 1 \end{bmatrix}$$

$$=\frac{1}{2}\begin{bmatrix} 1 & i & i & -1 \\ i & 1 & -1 & i \\ i & -1 & 1 & i \\ -1 & i & i & 1 \end{bmatrix} \quad \text{(I.34)}$$

The reciprocal of (I.34) is:

$$R_{90xCH}^{-1}=\frac{1}{2}\begin{bmatrix} 1 & -i & -i & -1 \\ -i & 1 & -1 & -i \\ -i & -1 & 1 & -i \\ -1 & -i & -i & 1 \end{bmatrix}$$

$$D(5)\cdot R_{90xCH}$$

$$=\frac{1}{2}\begin{bmatrix} 3-2i(c-is) & 3i+2(c-is) & 3i-2(c-is) & -3-2i(c-is) \\ 2i-2(c-is) & 2+2i(c-is) & -2+2i(c-is) & 2i+2(c-is) \\ 3i-2(c+is) & -3-2i(c+is) & 3-2i(c+is) & 3i+2(c+is) \\ -2+2i(c+is) & 2i+2(c+is) & 2i-2(c+is) & 2+2i(c+is) \end{bmatrix}$$

Premultiplying the last result by R_{90xCH}^{-1} gives

$$D(7)=\frac{1}{2}\begin{bmatrix} 5 & i-4is & 0 & -4ic \\ -i+4is & 5 & 4ic & 0 \\ 0 & -4ic & 5 & i+4is \\ 4ic & 0 & -i-4is & 5 \end{bmatrix} \qquad \text{(I.35)}$$

Comparing $D(7)$ with $D(5)$ we make two distinct observations. First, as expected, carbon coherences are created in d_{12} and d_{34} due to the $90xC$ pulse. Second, the proton information [$s = \sin\Omega_H(t_e + \Delta_1)$] has been transferred from d_{13} and d_{24} into the carbon coherences d_{12} and d_{34}, which are

$$d_{12}=\frac{i-4is}{2}$$

$$d_{34}=\frac{i+4is}{2}$$

This is an important point of the sequence because now the *mixed* carbon and proton information can be carried into the final FID.

3.9 The Role of Δ_2

As we will see soon, the observable signal is proportional to the sum $d_{12} + d_{34}$. If we started the decoupled acquisition right at $t(7)$, the terms containing s would be cancelled. To save them, we allow for one more short coupled evolution Δ_2. Since no r.f. pulse follows after $t(7)$, we know that every matrix element will evolve in its own box according to (I.13). It is therefore sufficient, from now on, to follow the evolution of the carbon coherences d_{12} and d_{34} which constitute the observables in this sequence.

According to (I.13), at $t(8)$ coherences d_{12} and d_{34} become

$$d_{12}(8) = i(1/2 - 2s)\exp(-i\Omega_{12}\Delta_2) \quad \text{(I.36)}$$
$$d_{34}(8) = i(1/2 + 2s)\exp(-i\Omega_{34}\Delta_2) \quad \text{(I.37)}$$

where $\Omega_{12} = \omega_{12} - \omega_{trC}$ and $\Omega_{34} = \omega_{34} - \omega_{trC}$ indicate that now we are in the carbon rotating frame, which is necessary to describe the carbon signal during the free induction decay.

As shown in Figure I.1 the transition frequencies of carbon (nucleus A) are:

$$\nu_{12} = \nu_A + \frac{J}{2} = \nu_C + \frac{J}{2}$$
$$\nu_{34} = \nu_A - \frac{J}{2} = \nu_C - \frac{J}{2}$$

Since $\omega = 2\pi\nu$, and we are in rotating coordinates we obtain:

$$\Omega_{12} = \Omega_C + \pi J \quad \text{(I.38)}$$
$$\Omega_{34} = \Omega_C - \pi J \quad \text{(I.39)}$$

Hence,

$$d_{12}(8) = i(1/2 - 2s)\exp(-i\Omega_C\Delta_2)\exp(-i\pi J\Delta_2) \quad \text{(I.40)}$$
$$d_{34}(8) = i(1/2 + 2s)\exp(-i\Omega_C\Delta_2)\exp(+i\pi J\Delta_2) \quad \text{(I.41)}$$

Analyzing the role of Δ_2 in (I.40 – 41) we see that for $\Delta_2 = 0$ the terms in s which contain the proton information are lost when we calculate the sum of d_{12} and d_{34} As discussed previously for Δ_1, here also, the desired signal is best obtained for $\Delta_2 = 1/2J$, which leads to $\exp(\pm i\pi J\Delta_2) = \pm i$ and

$$d_{12}(8) = +(1/2 - 2s)\exp(-i\Omega_C\Delta_2) \quad \text{(I.42)}$$
$$d_{34}(8) = -(1/2 + 2s)\exp(-i\Omega_C\Delta_2) \quad \text{(I.43)}$$

3.10 Detection

From the time $t(8)$, on the system is proton decoupled, i.e., both d_{12} and d_{34} evolve with the frequency Ω_C:

$$d_{12}(9) = +(1/2 - 2s)\exp(-i\Omega_C\Delta_2)\exp(-i\Omega_C t_d) \qquad \text{(I.44)}$$
$$d_{34}(9) = -(1/2 + 2s)\exp(-i\Omega_C\Delta_2)\exp(-i\Omega_C t_d) \qquad \text{(I.45)}$$

Our density matrix calculations, carried out for every step of the sequence, have brought us to the relations (I.44-45). Now it is time to derive the observable (transverse) carbon magnetization components. This is done by using the relations (B19) and (B20) in Appendix B:

$$M_{TC} = M_{xC} + iM_{yC} = -(4M_{oC}/p)(d_{12}^* + d_{34}^*) \qquad \text{(I.46)}$$

The transverse magnetization M_T is a complex quantity which combines the x and y components of the magnetization vector. We must now reintroduce the factor $p/4$ which we omitted, for convenience, starting with (I.7). This allows us to rewrite (I.46) into a simpler form:

$$M_{TC} = -M_{oC}(d_{12}^* + d_{34}^*) \qquad \text{(I.47)}$$

By inserting (I.44-45) into (I.47) we obtain

$$M_{TC} = 4M_{oC}s\exp(i\Omega_C\Delta_2)\exp(i\Omega_C t_d) \qquad \text{(I.48)}$$

With the explicit expression of s (I.31):

$$M_{TC} = 4M_{oC}\sin[\Omega_H(t_e + \Delta_1)]\exp(i\Omega_C\Delta_2)\exp(i\Omega_C t_d) \qquad \text{(I.49)}$$

Equation (I.49) represents the final result of our 2DHETCOR analysis by means of the density matrix formalism and it contains all the information we need.

We learn from (I.49) *that the carbon magnetization rotates by* $\Omega_C t_d$ *while being amplitude modulated by the proton evolution* $\Omega_H t_e$. *Fourier transformation with respect to both time domains will yield the two-dimensional spectrum.*

The signal is enhanced by a factor of four, representing the γ_H/γ_C *ratio. The polarization transfer achieved in* 2DHETCOR *and*

other heteronuclear pulse sequences cannot be explained by the vector representation.

When transforming with respect to t_d, all factors other than $\exp(i\Omega_C t_d)$ are regarded as constant. A single peak frequency, Ω_C, is obtained. When transforming with respect to t_e, all factors other than $\sin[\Omega_H(t_e + \Delta_1)]$ are regarded as constant. Since

$$\sin\alpha = \frac{e^{i\alpha} - e^{-i\alpha}}{2i} \tag{I.50}$$

both $+\Omega_H$ and $-\Omega_H$ are obtained (Figure I.3a).

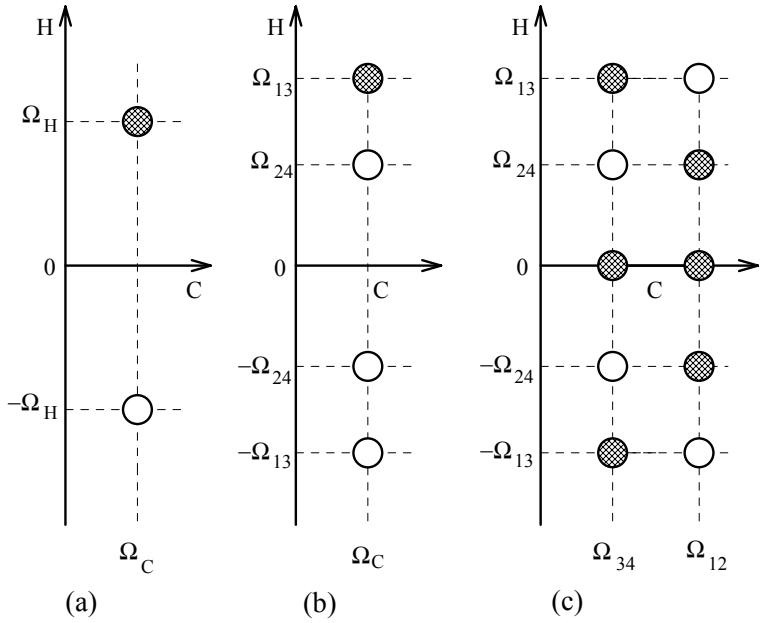

Figure I.3. Schematic 2D heteronuclear correlation spectra (contour plot): (a) fully decoupled, (b) proton decoupled during the acquisition, and (c) fully coupled. Filled and open circles represent positive and negative peaks. With the usually employed magnitude calculation (absolute value), all peaks are positive. See experimental spectra in figures 3.11, 3.9 and 3.7 of the book by Martin and Zektzer (see Suggested Readings).

Imagine now that in the sequence shown in Figure I.2 we did not apply the 180° pulse on carbon and suppressed Δ_1. During the evolution time t_e the proton is coupled to carbon. During the

acquisition, the carbon is decoupled from proton. The result (see Appendix I) is that along the carbon axis we see a single peak, while along the proton axis we see a doublet due to the proton-carbon coupling. If we calculate the magnetization following the procedure shown before, we find:

$$M_{TC} = -2\,M_{oC}(\cos\Omega_{13}t_e - \cos\Omega_{13}t_e)\exp[i\Omega_C(t_d + \Delta_2)] \qquad \text{(I.51)}$$

Reasoning as for (I.49) we can explain the spectrum shown in Figure I.3b.

Finally, if we also suppress the decoupling during the acquisition and the delay Δ_2 we obtain (see Appendix I)

$$\begin{aligned} M_{TC} = &-iM_{oC}(1/2 - \cos\Omega_{13}t_e + \cos\Omega_{24}t_e)\exp(i\Omega_{12}t_d) \\ &-iM_{oC}(1/2 + \cos\Omega_{13}t_e - \cos\Omega_{24}t_e)\exp(i\Omega_{34}t_d) \end{aligned} \qquad \text{(I.52)}$$

which yields the spectrum shown in Figure I.3c.

The lower part of the spectra is not displayed by the instrument, but proper care must be taken to place the proton transmitter beyond the proton spectrum. Such a requirement is not imposed on the carbon transmitter, provided quadrature phase detection is used.

The peaks in the lower part of the contour plot (negative proton frequencies) can also be eliminated if a more sophisticated pulse sequence is used, involving phase cycling. If such a pulse sequence is used, the proton transmitter can be positioned at mid-spectrum as well. An example of achieving quadrature detection in the domain t_e is given in Section 6 (COSY with phase cycling).

So far we have treated the AX (CH) system. In reality, the proton may be coupled to one or several other protons. In the sequence shown in Figure I.2 there is no proton-proton decoupling. The 2D spectrum will therefore exhibit single resonances along the carbon axis, but multiplets corresponding to proton-proton coupling, along the proton axis. An example is given in Figure I.4a which represents the high field region of the 2DHECTOR spectrum of a molecule

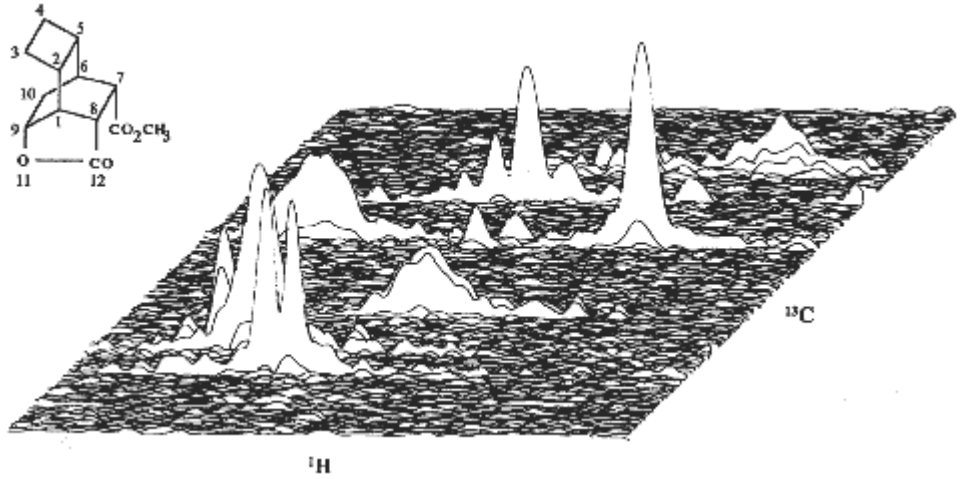

Figure I.4a. The high field region of the 2DHETCOR stack plot of a Nenitzescu's hydrocarbon derivative in $CDCl_3$ (at 50 MHz for ^{13}C). The peaks corresponding to the carbonyls, the methyl group, and the carbon in position 9 are at lower fields (M. Avram, G.D. Mateescu and C.D. Nenitzescu, unpublished work).

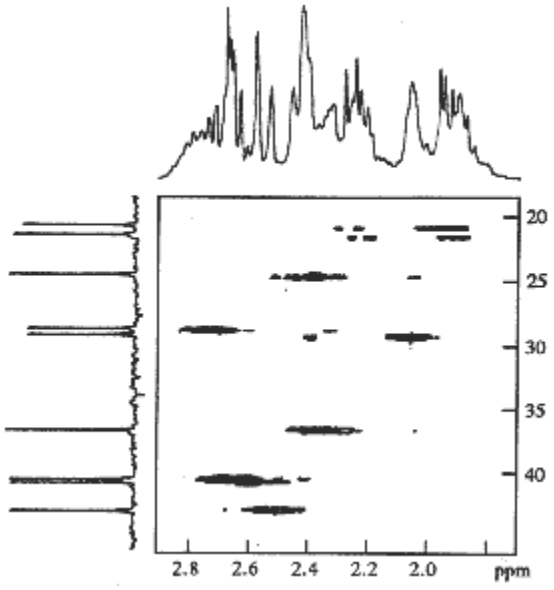

Figure I.4b. Contour plot of the spectrum in Figure I.4a.

formally derived from [4,2,2,$0^{2,5}$]deca-3,7,9-triene (Nenitzescu's hydrocarbon). The delays Δ_1 and Δ_2 were set to 3.6 ms in order to optimize the signals due to ^1J ($\cong$140 Hz). It should be noted that the relation (I.49) has been derived with the assumption that $\Delta_1 = \Delta_2 = \Delta = 1/2J$. For any other values of J the signal intensity is proportional to $\sin^2\pi J\Delta$. Thus, signals coming from long range couplings will have very small intensities. Figure I.4b is a contour plot of the spectrum shown in Figure I.4a. It shows in a more dramatic manner the advantage of 2D spectroscopy: the carbon-proton correlation and the disentangling of the heavily overlapping proton signals.